Acta Crystallographica Section F
Structural Biology and Crystallization Communications
ISSN 1744-3091

Expression, purification and preliminary crystallographic analysis of *Drosophila melanogaster* lysosomal α-mannosidase

I. Nemčovičová,[a,b]* M. Nemčovič,[b] S. Šesták,[b] M. Plšková,[b] I. B. H. Wilson[c] and J. Mucha[b]

[a]Department of Cellular Biology, La Jolla Institute for Allergy and Immunology, 9420 Athena Circle, La Jolla, CA 92037, USA, [b]Department of Glycobiology, Institute of Chemistry, Slovak Academy of Sciences, Dúbravská cesta 9, 845 38 Bratislava, Slovakia, and [c]Department für Chemie, Universität für Bodenkultur, Muthgasse 18, A-1190 Wien, Austria

Correspondence e-mail: tomiva@liai.org

Received 20 March 2012
Accepted 28 June 2012

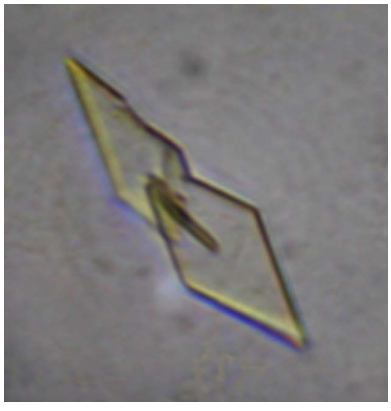

The lysosomal α-mannosidases are class II mannosidases that belong to glycoside hydrolase family 38 and play an important role in the degradation of asparagine-linked carbohydrates of glycoproteins. Based on peptide similarity to human and bovine lysosomal mannosidase (LM), recombinant α-mannosidase from *Drosophila melanogaster* (dLM408) was cloned and heterologously expressed in *Pichia pastoris*. The recombinant form of dLM408 designed for structural analysis lacks the transmembrane domain and was crystallized using standard vapour-diffusion and counter-diffusion techniques. The crystals grew as flat plates and as tetragonal bipyramids, respectively. The plate-shaped crystals exhibited the symmetry of space group $P2_12_12_1$ and diffracted to a minimum *d*-spacing of 3.5 Å.

1. Introduction

Carbohydrates are the most structurally diverse and complex biopolymers in biological systems. It has been predicted that 1% of the genes in the mammalian genome are involved in carbohydrate biosynthesis and modification (Lowe & Marth, 2003). Most extracellular proteins contain asparagine-linked (N-linked) oligosaccharides (N-linked glycans or N-glycans) as a result of post-translational modification. The carbohydrates attached to these different proteins have been found to influence interactions with their environment and many important biological events, including protein folding and localization, as well as to play important roles in cell–cell communication (Rastan *et al.*, 1985; Norgard *et al.*, 1993; Vallee *et al.*, 2000). The structural diversity and complexity of N-glycans allows the wide range of functions exhibited by these glycoconjugates and is essential for proper functioning in metazoan organisms.

Mannosidases involved in the biosynthesis and catabolism of N-glycans have been divided into several broad classes based on sequence comparisons, specificity for substrates and other characteristics. Class II mannosidases belong to glycosyl hydrolase family 38 (GH38; Henrissat & Bairoch, 1996) and are comprised of a group of enzymes that cleave mannose residues from the nonreducing termini of N-glycans during biosynthesis in the ER and Golgi complex and catabolism in the lysosomes and cytosol. Class II mannosidases are defined by a relatively large protein molecular weight (110–135 kDa), sensitivity to furanose transition-state analogues such as swainsonine and 1,4-dideoxy-1,4-imino-D-mannitol, a varying cation requirement for Zn^{2+} or Co^{2+}, an ability to cleave glycosidic linkages by a retaining enzymatic mechanism and a region of conserved sequence predominantly associated with the catalytic domain residues (Henrissat & Bairoch, 1993, 1996; Henrissat & Davies, 1997; Bourne & Henrissat, 2001). Each enzyme in this class can be differentiated by its distinctive features of localization in the cell, optimum pH, substrate specificity and metal-ion requirement. In mammals there are at least five different class II mannosidases. The first enzyme is Golgi mannosidase II (GMII). This enzyme is involved in the cleavage of $GlcNAcMan_5GlcNAc_2$ to $GlcNAcMan_3GlcNAc_2$ in glycoprotein biosynthesis, has a pH optimum of around 5.5, is stimulated by zinc and is localized to Golgi membranes (Tabas & Kornfeld, 1978; Harpaz & Schachter, 1980; Tulsiani *et al.*, 1982; Moremen *et al.*, 1991). The protein structure of *Drosophila melanogaster* Golgi mannosidase II (dGMII) has been reported by van den

Elsen *et al.* (2001). The second enzyme is a GMII homologue that is called Golgi mannosidase IIx (GMIIx; Misago *et al.*, 1995). This enzyme is involved in glycan processing in the Golgi complex of cells, has a pH optimum of around 5.5 and is thought to be an alternative route to complex N-linked glycosylation in the absence of GMII (Chui *et al.*, 1997; Oh-Eda *et al.*, 2001; Hato *et al.*, 2006); it appears to have a similar substrate specificity to GMII. The third enzyme is the broad-specificity lysosomal α-mannosidase (LM), a catabolic mannosidase with a broad substrate specificity and low pH optimum (∼4.5) that is found in the lysosomes of cells (al Daher *et al.*, 1991; Daniel *et al.*, 1994; Liao *et al.*, 1996; Merkle *et al.*, 1997). The protein structure of bovine (*Bos taurus*) lysosomal mannosidase (bLM) has been solved, but at a pH at which the protein was not active (Heikinheimo *et al.*, 2003). The fourth enzyme is a lysosomal core-specific α-1,6-mannosidase with a low pH optimum (∼4.0) that is involved in catabolism of glycans in the lysosomes (Park *et al.*, 2005). The fifth class II enzyme is a soluble or cytoplasmic mannosidase that is a catabolic mannosidase with a neutral pH optimum (∼6.5); it is stimulated by Co^{2+} and is found in the cytosol of mammalian cells (Shoup & Touster, 1976; Bischoff *et al.*, 1990). A proteolytically cleaved form of this enzyme has been detected in the ER and is thought to be involved in the early steps of glycoprotein biosynthesis (Weng & Spiro, 1993, 1996).

The most extensively studied of these enzymes is the *Drosophila* GH38 α-mannosidase II, which has been shown to be a retaining α-mannosidase that targets both α-1,3-mannosyl and α-1,6-mannosyl linkages, an activity that enables the enzyme to process GlcNAc $(Man)_5(GlcNAc)_2$ hybrid N-glycans to $GlcNAc(Man)_3(GlcNAc)_2$ (Fig. 1). Far less understood is the observation that many bacterial species, predominantly but not exclusively pathogens and symbionts, also possess putative GH38 α-mannosidases whose activity and specificity is unknown.

In this report, we studied lysosomal α-mannosidase (LM; EC 3.2.1.24), which is a major exoglycosidase in the glycoprotein-degradation pathway. In humans, cattle, cats and guinea pigs, lack of this lysosomal α-mannosidase activity causes the autosomal recessive disease α-mannosidosis. Recently, great progress has been made in studying the enzyme and its deficiency (Sun & Wolfe, 2001). This includes cloning of the gene encoding the enzyme, the characterization of mutations related to disease, the establishment of valuable animal models *etc.* Moreover, swainsonine, a plant-derived indolizidine alkaloid, has been found to be a potent inhibitor of GMII, with a K_i of 40 n*M* against the *D. melanogaster* enzyme (dGMII; Shah *et al.*, 2003). Clinical trials have suggested that swainsonine has therapeutic value because it reduces metastasis and improves clinical outcome in cancers of the colon, breast and skin (Goss *et al.*, 1997; Baptista *et al.*, 1994). Unfortunately, there are side effects resulting from swainsonine treatment because it also inhibits a structurally related lysosomal mannosidase involved in catabolic processes which is of interest to us. To date only one protein structure of lysosomal mannosidase (cloned from *B. taurus*) has been solved, but at a pH at which the protein was not active (Heikinheimo *et al.*, 2003). Therefore, the determination of the structure of *D. melanogaster* lysosomal α-mannosidase (dLM408) under active conditions will help in understanding the catalytic process of both Golgi and lysosomal mannosidases and will allow the development of highly specific inhibitors and thus more efficacious chemotherapeutics. Furthermore, it will help in understanding the human form of α-mannosidosis. Here, we report our recent findings on dLM408, including its characterization, expression, purification, crystallization and preliminary X-ray diffraction analysis.

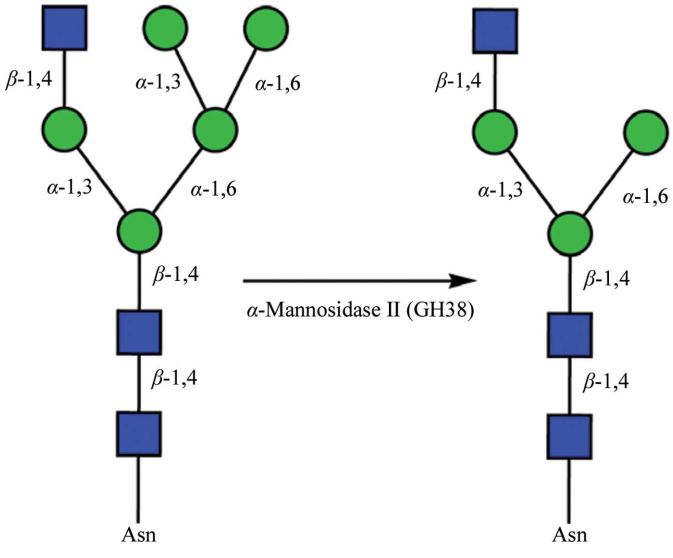

Figure 1
Catalytic activity of GH38 α-mannosidase II. The schematic illustration shows the process of the hydrolysis of both α-1,3-mannosides and α-1,6-mannosides during the diversification of hybrid N-glycans (conversion of $GlcNAcMan_5GlcNAc_2$ to $GlcNAcMan_3GlcNAc_2$).

2. Materials and methods

2.1. Activity assay

As reported previously (Poláková *et al.*, 2011), dLM408 can hydrolyze *p*-nitrophenyl α-mannopyranoside (pNP-α-Man) and is inhibited by swainsonine and mannostatin A (data not shown). The substrate specificity of this enzyme during the time course of expression and purification was determined using oligomannosidic $Man_{8-9}GlcNAc_2$ N-glycans and the activity of dLM408 was determined by the standard α-mannosidase activity assay reported previously (Poláková *et al.*, 2011). Briefly, the supernatant from yeast expressing a soluble form of dLM408 was incubated with the substrate pNP-α-Man at 310.15 K for 2–3 h. The standard assay mixture consisted of 50 m*M* sodium acetate buffer pH 5.2, 2 m*M* pNP-α-Man (from 100 m*M* stock solution in DMSO) and 1–5 µl enzyme (the supernatant of the culture medium) in a total reaction volume of 50 µl. A blank sample contained no enzyme. The samples were prepared as duplicates. The reactions were terminated by the addition of 500 µl 100 m*M* Na_2CO_3 and the absorbance was recorded at 410 nm using a spectrophotometer.

2.2. Protein expression and purification

We cloned the corresponding DNA fragment encoding residues 34–1080 of dLM408 (NCBI reference NP_609408.1) into modified expression vector pICZα (Invitrogen) under the precise control of the *AOX1* induction promoter. The expression construct further contains uncleavable affinity epitopes, including a six-His tag and a FLAG-tag. Prior to crystallographic study, the N-terminally tagged form of dLM408 was heterologously expressed in the methylotrophic yeast *Pichia pastoris* strain GS115 (Invitrogen). Optimal expression was achieved in MMYC medium at 291.15 K with methanol induction over 3 d. After expression in yeast, dLM408 activity was determined by a standard α-mannosidase activity assay (see §2.1) using synthetic pNP-α-Man as a substrate. The first step in isolating recombinant dLM408 from bulk yeast culture was precipitation with ammonium sulfate. This was performed by adding increasing amounts of ammonium sulfate [up to 75%(*w*/*v*)] and collecting the different

fractions of precipitated protein. These fractions were resuspended in 50 m*M* Tris pH 8.5 containing 300 m*M* NaCl. Ammonium sulfate was then removed by dialysis against 50 m*M* Tris pH 8.5 containing 300 m*M* NaCl, 5 m*M* imidazole, 0.1%(*v*/*v*) Triton X-100 (the binding buffer for subsequent affinity purification). The elution of His-tagged dLM408 from the Ni–NTA agarose column was performed in several steps to achieve a concentration gradient of imidazole from 20 m*M* (washing step) to 300 m*M*. Eluted dLM408 was dialyzed against 50 m*M* HEPES pH 7.5, 150 m*M* NaCl to remove residual imidazole. After final purification, the activity of the enzyme was determined by mannosidase assay and the purity of dLM408 was analyzed by SDS–PAGE. The molecular weight of the purified N-terminally tagged dLM408 was estimated by SDS–PAGE analysis (Fig. 2) and the final concentration of the enzyme was determined by the Bradford method (Bradford, 1976).

2.3. Crystallization of dLM408

Prior to crystallization experiments using the recombinant dLM408 (including both a His tag and a FLAG-tag), the enzyme was deglycosylated by PNGase F (Invitrogen) and the buffer was changed to 50 m*M* HEPES pH 6.8, 150 m*M* NaCl by concentration or dialysis at 277.15 K. The protein concentration in all crystallization trials varied between 5 and 10 mg ml^{-1}. Crystallization conditions were initially screened by means of the counter-diffusion method (García-Ruiz, 2003; Otálora *et al.*, 2009) using the Counterdiffusion Screening Kit (GCB-CSK-24) for protein crystallization (Triana Science and Technology, Granada, Spain). Each kit consisted of 24 GCB-Domino boxes pre-filled with precipitant solution buffered at different pH values and agarose. The protein solution containing dLM408 was used to fill 0.1 mm diameter capillaries, which were sealed with wax at the top of the capillary. One 0.1 mm capillary was then punched into the agarose in each GCB-Domino box. The initial crystallization hit (condition C3) yielded microcrystals that were unusable for diffraction measurement. We further optimized this condition using the vapour-diffusion method, in which 2 µl protein solution was premixed with 2 µl precipitating solution (reservoir solution) and placed on a glass cover slip or as a sitting drop over a reservoir consisting of 30%(*v*/*v*) PEG 8000, 50 m*M* sodium cacodylate, 150 m*M* sodium acetate in the pH range 5–6. In addition, the same protein solution containing dLM408 and the same precipitating agent at a lower pH (from 4.5 to 5) was used to fill 0.1–0.2 mm diameter capillaries. This standard counter-diffusion technique was arranged such that the volumes of the precipitating agent and protein solution were juxtaposed with one another inside the capillary. These two solutions were set to diffuse against each other, resulting in a spatial–temporal

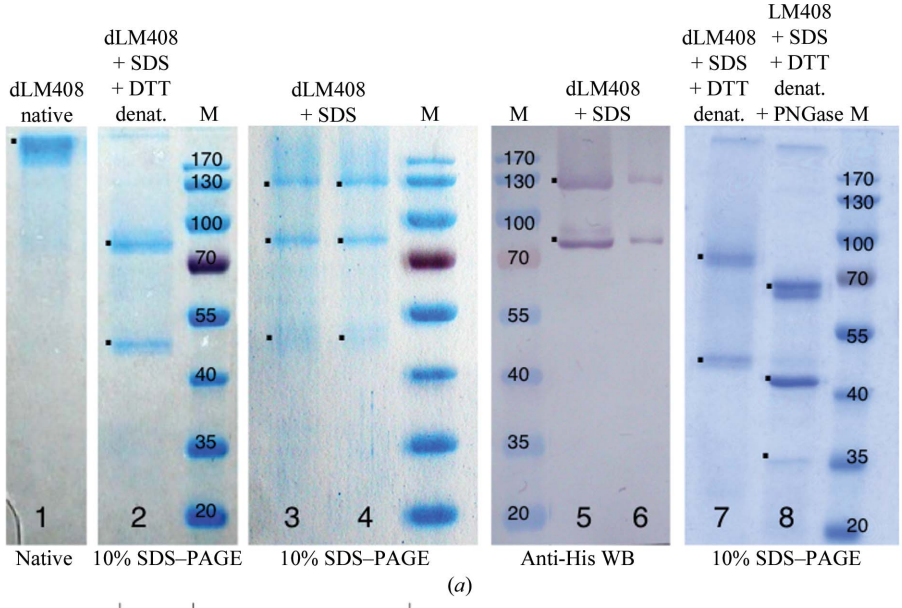

34–1080	1046	dLM408 full length
34–327	293	dLM408 a-peptide
328–409	81	dLM408 b-peptide
410–598	188	dLM408 c-peptide
599–886	287	dLM408 d-peptide
887–1080	193	dLM408 e-peptide

(*b*)

Figure 2
(*a*) Analysis of purified recombinant lysosomal α-mannosidaze (dLM408) on a native gel (lane 1), 10% SDS–PAGE (lanes 2, 3, 4, 7 and 8) and a Western blot (lanes 5 and 6). The uppermost protein band in the first lane corresponds to recombinant dLM408 purified under the native conditions (lane 1). The next three lanes correspond to the same purified sample of dLM408 under heat-denatured reducing conditions (lane 2) and nonreducing conditions (lanes 3 and 4). The two upper bands of dLM408 were also detected by the Western blot technique using anti-His antibodies (lanes 5 and 6). PNGase treatment of dLM408 was followed by running samples on 10% SDS–PAGE under heat-denatured reducing conditions (lane 8). Lane 7 contains untreated control sample. Lanes M contain molecular-weight markers (labelled in kDa). (*b*) Peptides originating from dLM408.

supersaturation gradient along the length of the capillary. Prior to mounting in cryoloops, the crystals obtained in capillaries were carefully transferred to a sitting drop and soaked in 30%(*v*/*v*) glycerol mixed with mother liquor.

2.4. Preliminary X-ray diffraction data collection and processing

In order to collect data at cryogenic temperature, both crystal forms that had been soaked in cryoprotectant [30%(*v*/*v*) glycerol in mother liquor] were cooled in liquid nitrogen, mounted on the goniostat under a nitrogen-gas stream at 100 K and tested for diffraction. X-ray diffraction measurements were performed remotely on beamline 7.1 at Stanford Synchrotron Radiation Laboratory (SSRL). A complete data set was collected from a plate-like crystal of dLM408 to 3.5 Å resolution using an X-ray wavelength of 1.2389 Å. For this data set, 260 frames of 10 s exposure time and 1° oscillation were collected. The distance between the crystal and the detector was maintained at 450 mm. A summary of the X-ray crystallographic data-collection statistics is given in Table 1. The data were indexed and processed with *iMOSFLM* (Battye *et al.*, 2011) as part of the *CCP*4 software suite (Winn *et al.*, 2011). The structure of dLM408 could be solved by the molecular-replacement method using the structure of bovine lysosomal α-mannosidase (PDB entry 1o7d; Heikinheimo *et al.*, 2003) as a search model.

3. Results

A search of GenBank for *D. melanogaster* proteins using bovine lysosomal α-mannosidase led to the retrieval of seven putative mannosidase homologues. Their sequence alignment indicated conservation of the catalytic nucleophile typical of class II mannosidases. The further conserved N-glycosylation consensus site (Asn489) with its two proximate cysteines (Cys485 and Cys493; see Supplementary Fig. 1[1] for a sequence alignment of insect, human and bovine lysosomal α-mannosidases) is typical for maintenance of lysosomal stability. In this study, we cloned and characterized a cDNA encoding class II lysosomal α-mannosidase from the dipteran insect *D. melanogaster* (dLM408; UniProtKB reference Q9VKV1; NCBI reference NP_609408.1, GH02419, isoform A; ORF name CG6206). dLM408 is a member of the GH38 α-mannosidase family, which has a PFAM signature peptide sequence in the amino-terminal region of the protein. This motif has been identified in *D. melanogaster*, *Spodotera frugiperda* and *Caenorhabditis elegans*, as well as bacterial, archaeal, fungal, mouse and human sequences. The amino-acid sequence of this enzyme is similar to those of various mammalian Golgi α-mannosidases II (GMIIs). Like other mannosidase enzymes, the *Drosophila* lysosomal α-mannosidase is an integral membrane glycoprotein with type II topology.

After expression in yeast, recombinant dLM408 showed significant activity using synthetic pNP-α-Man as a substrate in the pH range 4.0–6.0, while the optimum reaction was at approximately pH 5.0 over the temperature range tested (298.15–313.15 K). As reported previously (Poláková *et al.*, 2011) and from our recent findings (data not shown), the K_m value for pNP-α-Man was in the range 1–2 m*M* and recombinant dLM408 was found to be reversibly inhibited by the glycoprotein-processing inhibitors swainsonine and mannostatin A in the nanomolar and micromolar ranges, respectively, further supporting its characterization as a class II α-mannosidase.

[1] Supplementary material has been deposited in the IUCr electronic archive (Reference: GJ5104).

Table 1
X-ray diffraction data-collection statistics for plate-like crystals of dLM408.

Values in parentheses are for the highest resolution shell.

X-ray source	Beamline 7-1, SSRL
Data-collection temperature (K)	100
Wavelength (Å)	1.2389
No. of images	260
Oscilation range (°)	1
Exposure time (s)	10
Space group	$P2_12_12_1$
Unit-cell parameters (Å, °)	a = 66.22, b = 92.63, c = 102.91, $\alpha = \beta = \gamma = 90$
No. of reflections	50888 (6830)
No. of unique reflections	10824 (1474)
Resolution limits (Å)	50.00–3.50 (3.75–3.50)
Mean $I/\sigma(I)$	11.6 (2.1)
Completeness (%)	98.7 (96.6)
R_{merge}† (%)	11.0 (26.2)

† $R_{merge} = \sum_{hkl}\sum_i |I_i(hkl) - \langle I(hkl)\rangle| / \sum_{hkl}\sum_i I_i(hkl)$, where $I_i(hkl)$ is the ith observation of reflection hkl and $\langle I(hkl)\rangle$ is the weighted average intensity for all i observations of reflection hkl.

The recombinant dLM408 enzyme was observed to be post-translationally processed into multiple peptide forms. SDS–PAGE analysis (Fig. 2) and deglycosylation studies confirmed occupation of the N-linked glycosylation sites and possible dimerization of the molecule. Two major bands (at 85 and 132 kDa) and one very faint band (at 47 kDa) were detected on SDS–PAGE in the absence of heat denaturation (Fig. 2*a*, lanes 3 and 4; both 5 µg), while the enzyme activity was only localized to the two upper bands (Fig. 2*a*, lanes 3 and 4), as well as to the uppermost band in the native gel (Fig. 2*a*, lane 1). No α-mannosidase activity was associated with the other bands in these lanes, indicating that they are likely to be contaminating polypeptides. On heat denaturation, the upper band disappeared and we observed two peptides with apparent masses of 85 and 47 kDa (Fig. 2*a*, lane 2). As these two peptides originated from the active dLM408 (band at 132 kDa), they probably constituted noncovalently linked peptides within the dLM408 complex. These two peptides revealed similar sizes to those of bovine and feline LM peptides referred to as the abc-peptide and the d-peptide, respectively. Furthermore, specific anti-His antibodies cross-reacted with the 132 and 85 kDa peptides (Fig. 2*a*, lanes 5 and 6), supporting the idea that the 85 kDa peptide constituted the N-terminal abc-peptide (Fig. 2*a*, lanes 5 and 6, lower band) and the 47 kDa peptide was the d-peptide. The e-peptides of about 13–20 kDa commonly found in human and bovine LMs originate from the C-terminal part of the single-chain LM precursor in these species (Tollersrud *et al.*, 1997; Nilssen *et al.*, 1997). The e-peptide was not found in our dLM408 sample. PNGase F (Invitrogen) treatment reduced the molecular masses of the 85 kDa peptide (abc-peptide) and the 47 kDa peptide (d-peptide) to 66 and 42 kDa, respectively (Fig. 2*a*, lanes 7 and 8), indicating that each of the two peptides was glycosylated. Molecular weights for purified N-terminally tagged dLM408 of about 95 kDa (deglycosylated) and 132 kDa (fully glycosylated) were estimated from the SDS–PAGE analysis (Fig. 2).

dLM408 crystals suitable for X-ray diffraction measurements were grown at room temperature (296.15 K) by vapour diffusion (Fig. 3*a*) as well as by the standard counter-diffusion crystallization technique (Fig. 3*b*). Optimized crystals were obtained using both the above-mentioned crystallization methods after several days using the following conditions: 30%(*v*/*v*) PEG 8000, 150 m*M* sodium acetate, 50 m*M* sodium cacodylate pH 4.5–6.0. The observed resolution of the plate-like dLM408 crystals was not better than 3.5 Å and the tetragonal bipyramid crystals diffracted even more weakly (∼7 Å). However, the dLM408 plate-like crystals were found to belong to the

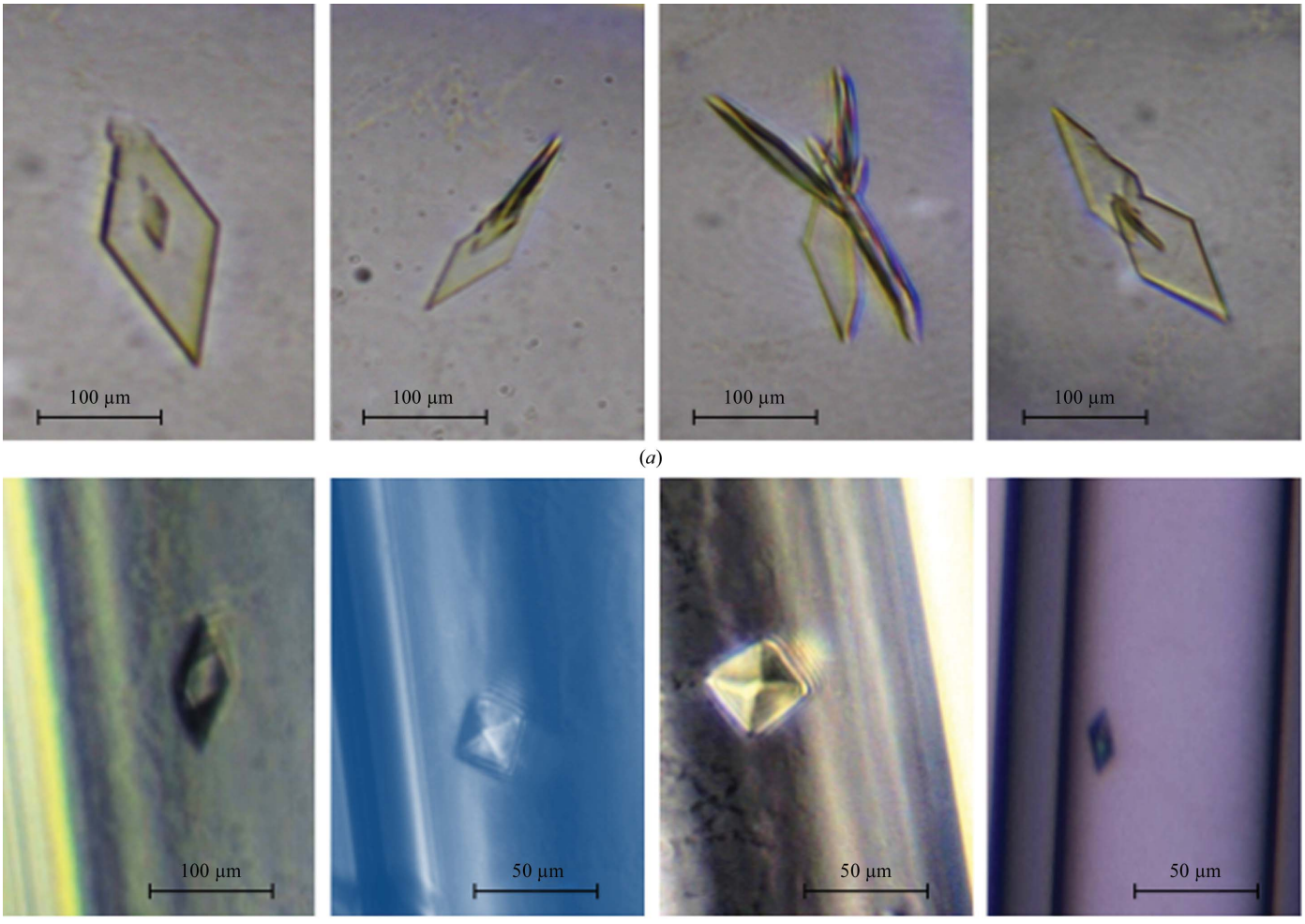

Figure 3
Crystals of dLM408 (lysosomal α-mannosidase II from *D. melanogaster*) grown by two different methods. (*a*) The sitting-drop and hanging-drop vapour-diffusion crystallization techniques yielded thin plate-shaped crystals; (*b*) crystals of tetragonal bipyramid shape were grown in capillaries using the standard counter-diffusion crystallization technique.

orthorhombic space group $P2_12_12_1$ (Fig. 3*a*, first on the left), with unit-cell parameters a = 66.2, b = 92.6, c = 102.9 Å. Calculation of the Matthews coefficient (V_M = 1.66 Å^3 Da^{-1}; 26% solvent content) indicated the presence of only one molecule per asymmetric unit (Matthews, 1968).

4. Discussion

We have shown that the *D. melanogaster* lysosomal mannosidase (dLM408) is an approximately 132 kDa enzyme with characteristics similar to those of other enzymes in the GH38 α-mannosidase family. These characteristics include a relatively large protein molecular weight (Fig. 2), a region of conserved sequence predominantly associated with catalytic domain residues (Suplementary Fig. 1), the ability to cleave mannose residues from the nonreducing terminus of N-glycans (Fig. 1 and data not shown), sensitivity to furanose transition-state analogues such as swainsonine and mannostatin A (Poláková *et al.*, 2011) and the requirement for a cation (Zn^{2+}) for catabolism (data not shown). In this manuscript, we have described the expression, purification and crystallization of the fruit-fly lysosomal α-mannosidase (dLM408) and the preliminary X-ray diffraction analysis of two forms of dLM408 crystals. One of the crystal forms offered promising structural data, while structural analysis at 3.5 Å resolution and the optimization of the second crystal form are currently under way. To the best of our knowledge, only one protein structure of lysosomal mannosidase (cloned from *B. taurus*) has been solved to date, but at a pH at which the protein was not active (Heikinheimo *et al.*, 2003). Therefore, we present here the successful crystallization of the first fly GH38 lysosomal enzyme, which offers indications for further biochemical studies of the family 38 glycoside hydrolases as well as lysosomal transport. Understanding the targeting and stability of lysosomal proteins and the biochemical background of inherited lysosomal disorders is of great interest to us. Therefore, determination of the dLM408 structure in its active form will help in understanding the catalytic processes of both Golgi and lysosomal mannosidases and will allow the development of highly specific inhibitors and thus more efficacious chemotherapeutics.

This work was supported by the Slovak Research and Development Agency APVV (0117-06), the Ministry of Education of the Slovak Republic and the Slovak Academy of Sciences – VEGA (2/0176/11) and the Austrian Fonds zur Förderung der wissenschaftlichen Forschung (L314). We thank the Stanford Synchrotron Radiation Laboratory for remote access to beamline 7.1 located at

Menlo Park, California, USA. IN and MN are also grateful to the organizers of the Fourth FEBS Advanced Crystallization Course held in Nové Hrady (Czech Republic) in 2010 for the opportunity to screen initial crystallization conditions using the broad collection of commercial crystallization kits available during this course.

References

al Daher, S., de Gasperi, R., Daniel, P., Hall, N., Warren, C. D. & Winchester, B. (1991). *Biochem. J.* **277**, 743–751.
Baptista, J. A., Goss, P., Nghiem, M., Krepinsky, J. J., Baker, M. & Dennis, J. W. (1994). *Clin. Chem.* **40**, 426–430.
Battye, T. G. G., Kontogiannis, L., Johnson, O., Powell, H. R. & Leslie, A. G. W. (2011). *Acta Cryst.* D**67**, 271–281.
Bischoff, J., Moremen, K. & Lodish, H. F. (1990). *J. Biol. Chem.* **265**, 17110–17117.
Bourne, Y. & Henrissat, B. (2001). *Curr. Opin. Struct. Biol.* **11**, 593–600.
Bradford, M. M. (1976). *Anal. Biochem.* **72**, 248–254.
Chui, D., Oh-Eda, M., Liao, Y.-F., Panneerselvam, K., Lal, A., Marek, K. W., Freeze, H. H., Moremen, K. W., Fukuda, M. N. & Marth, J. D. (1997). *Cell*, **90**, 157–167.
Daniel, P. F., Winchester, B. & Warren, C. D. (1994). *Glycobiology*, **4**, 551–566.
Elsen, J. M. van den, Kuntz, D. A. & Rose, D. R. (2001). *EMBO J.* **20**, 3008–3017.
García-Ruiz, J. M. (2003). *Methods Enzymol.* **368**, 130–154.
Goss, P. E., Reid, C. L., Bailey, D. & Dennis, J. W. (1997). *Clin. Cancer Res.* **3**, 1077–1086.
Harpaz, N. & Schachter, H. (1980). *J. Biol. Chem.* **255**, 4894–4902.
Hato, M., Nakagawa, H., Kurogochi, M., Akama, T. O., Marth, J. D., Fukuda, M. N. & Nishimura, S. (2006). *Mol. Cell. Proteomics*, **5**, 2146–2157.
Heikinheimo, P., Helland, R., Leiros, H. K. S., Leiros, I., Karlsen, S., Evjen, G., Ravelli, R., Schoehn, G., Ruigrok, R., Tollersrud, O. K., McSweeney, S. & Hough, E. (2003). *J. Mol. Biol.* **327**, 631–644.
Henrissat, B. & Bairoch, A. (1993). *Biochem. J.* **293**, 781–788.
Henrissat, B. & Bairoch, A. (1996). *Biochem. J.* **316**, 695–696.
Henrissat, B. & Davies, G. (1997). *Curr. Opin. Struct. Biol.* **7**, 637–644.
Liao, Y.-F., Lal, A. & Moremen, K. W. (1996). *J. Biol. Chem.* **271**, 28348–28358.
Lowe, J. B. & Marth, J. D. (2003). *Annu. Rev. Biochem.* **72**, 643–691.
Matthews, B. W. (1968). *J. Mol. Biol.* **33**, 491–497.
Merkle, R. K., Zhang, Y., Ruest, P. J., Lal, A., Liao, Y.-F. & Moremen, K. W. (1997). *Biochim. Biophys. Acta*, **1336**, 132–146.
Misago, M., Liao, Y.-F., Kudo, S., Eto, S., Mattei, M. G., Moremen, K. W. & Fukuda, M. N. (1995). *Proc. Natl Acad. Sci. USA*, **92**, 11766–11770.
Moremen, K. W., Touster, O. & Robbins, P. W. (1991). *J. Biol. Chem.* **266**, 16876–16885.
Nilssen, O., Berg, T., Riise, H. M., Ramachandran, U., Evjen, G., Hansen, G. M., Malm, D., Tranebjaerg, L. & Tollersrud, O. K. (1997). *Hum. Mol. Genet.* **6**, 717–726.
Norgard, K. E., Moore, K. L., Diaz, S., Stults, N. L., Ushiyama, S., McEver, R. P., Cummings, R. D. & Varki, A. (1993). *J. Biol. Chem.* **268**, 12764–12774.
Oh-Eda, M., Nakagawa, H., Akama, T. O., Lowitz, K., Misago, M., Moremen, K. W. & Fukuda, M. N. (2001). *Eur. J. Biochem.* **268**, 1280–1288.
Otálora, F., Gavira, J. A., Ng, J. D. & García-Ruiz, J. M. (2009). *Prog. Biophys. Mol. Biol.* **101**, 26–37.
Park, C., Meng, L., Stanton, L. H., Collins, R. E., Mast, S. W., Yi, X., Strachan, H. & Moremen, K. W. (2005). *J. Biol. Chem.* **280**, 37204–37216.
Poláková, M., Šesták, S., Lattová, E., Petruš, L., Mucha, J., Tvaroška, I. & Kóňa, J. (2011). *Eur. J. Med. Chem.* **46**, 944–952.
Rastan, S., Thorpe, S. J., Scudder, P., Brown, S., Gooi, H. C. & Feizi, T. (1985). *J. Embryol. Exp. Morphol.* **87**, 115–128.
Shah, N., Kuntz, D. A. & Rose, D. R. (2003). *Biochemistry*, **42**, 13812–13816.
Shoup, V. A. & Touster, O. (1976). *J. Biol. Chem.* **251**, 2845–3852.
Sun, H. & Wolfe, J. H. (2001). *Exp. Mol. Med.* **33**, 1–7.
Tabas, I. & Kornfeld, S. (1978). *J. Biol. Chem.* **253**, 7779–7786.
Tollersrud, O. K., Berg, T., Healy, P., Evjen, G., Ramachandran, U. & Nilssen, O. (1997). *Eur. J. Biochem.* **246**, 410–419.
Tulsiani, D. R., Harris, T. M. & Touster, O. (1982). *J. Biol. Chem.* **257**, 7936–7939.
Vallee, F., Karaveg, K., Herscovics, A., Moremen, K. W. & Howell, P. L. (2000). *J. Biol. Chem.* **275**, 41287–41298.
Weng, S. & Spiro, R. G. (1993). *J. Biol. Chem.* **268**, 25656–25663.
Weng, S. & Spiro, R. G. (1996). *Arch. Biochem. Biophys.* **325**, 113–123.
Winn, M. D. *et al.* (2011). *Acta Cryst.* D**67**, 235–242.